Exchange Energy Formulations for 3D Micromagnetics

M. J. Donahue and D. G. Porter

Abstract—**Exchange energy is especially sensitive to the numerical representation selected. We compare three discretized exchange energy formulations for 3D numerical micromagnetics on rectangular grids. Explicit formulae are provided for both Neumann and Dirichlet boundary conditions. Results illustrate the convergence order of these methods as a function of discretization cell size and the effect of cell size on vortex pinning.**

Keywords: micromagnetics, exchange, convergence

I. Introduction

In the continuum theory that underlies micromagnetics, the term representing the quantum mechanical exchange interaction can be written as

$$E_{\text{ex}} = \int_V A \left(|\nabla m_x|^2 + |\nabla m_y|^2 + |\nabla m_z|^2 \right) \, dV, \quad (1)$$

where A is the exchange coefficient and $\mathbf{m} = (m_x, m_y, m_z)$ represents the reduced magnetization, $\mathbf{M}/M_s$. It follows from the constraint $\|\mathbf{m}\|^2 = 1$ that $\mathbf{m} \cdot \partial \mathbf{m}/\partial x = 0$, and similarly for $\partial/\partial y$ and $\partial/\partial z$. This combines with the general relation $|\nabla f|^2 = \nabla \cdot (f \nabla f) - f \nabla^2 f$ to show that (1) can be rewritten as

$$E_{\text{ex}} = -\int_V A \, \mathbf{m} \cdot \left(\frac{\partial^2 \mathbf{m}}{\partial x^2} + \frac{\partial^2 \mathbf{m}}{\partial y^2} + \frac{\partial^2 \mathbf{m}}{\partial z^2} \right) \, dV. \quad (2)$$

A numerical implementation of micromagnetics must utilize a discretized form of (1) or (2). The order of a numerical method is defined as the rate at which the error decreases as the discretization cell size h tends to 0. For example, if there is a constant B such that the error is smaller than Bh^2 as $h \to 0$, we say the error is $O(h^2)$, or that the method is second order. There are many factors to consider when selecting a numerical implementation, such as method order, boundary conditions, and seriousness of discretization induced artifacts like vortex pinning [1]. In this work we analyze three discretization methods on rectangular lattices, involving 6, 12, and 26 neighbors, with two types of boundary conditions.

The authors are with the National Institute of Standards and Technology, Gaithersburg, MD 20899, USA. E-mail: michael.donahue@nist.gov

II. Theory

Evaluating either (1) or (2) numerically involves evaluating both the integral and the enclosed derivative. Additionally, special handling of the derivative is required at the boundary of the simulation region. In order to obtain a specified method order, say $O(h^4)$, each step must retain at least that accuracy.

A. Integration techniques

A one-dimensional integral can be approximated by the discrete sum

$$\int_a^b f(x) \, dx = h \sum_{k=1}^n w_k f_k + O(h^\alpha),$$

where $f_k = f(x_k)$ at sample points $x_k = a + (k - 1/2)h$, $h = (b - a)/n$ is the distance between successive samples, (w_k) is a collection of weights, and α is the method order. In this discretization the sample points are all interior to the interval $[a, b]$. It is easy to show [2] that the simple sum with all $w_k = 1$ is $O(h^2)$ provided that f is twice continuously differentiable, i.e., $f \in C^2[a, b]$.

In general, to obtain a higher order method one must vary the weights w_k. Simpson's rule, with weights $1, 4, 2, 4, \ldots, 2, 4, 1$, is a well known $O(h^4)$ method for the case where the samples x_k include the endpoints a and b. There are also methods where the w_k's are identically 1 in the interior, and vary only at the ends [3]. Using the methods in [2], [3], one can show that the weights

$$(w_k) = \frac{26}{24}, \frac{21}{24}, \frac{25}{24}, 1, 1, \ldots, 1, \frac{25}{24}, \frac{21}{24}, \frac{26}{24} \quad (3)$$

yield an $O(h^4)$ integration method for $f \in C^4[a, b]$.

A three dimensional integral can be obtained by iterating the above method,

$$\int_V f \, dV = V_h \sum_{ijk} w_i^x w_j^y w_k^z f_{ijk} + O(h^4), \quad (4)$$

where $V_h = h_x h_y h_z$ is an individual cell volume, with h_x, h_y, h_z the sample periods along the x, y and z axes, respectively, w_i^x, w_j^y, w_k^z are the weights (3) extended to fit the sample sequences along the corresponding axes, f_{ijk} is the value of f at point (x_i, y_j, z_k), and $h = \max(h_x, h_y, h_z)$.

B. 6- and 12-neighbor methods

If we consider one term in (2), say

$$\Phi = -\int_V A\,\mathbf{m} \cdot \frac{\partial^2 \mathbf{m}}{\partial x^2}\,dV, \tag{5}$$

then Φ can be represented numerically as

$$\Phi_{\mathrm{d}} = -V_h \sum_{jk} w_j^y w_k^z \sum_{ii'} A_{ijk} w_i^x\, d_{ii'}\, \mathbf{m}_{ijk} \cdot \mathbf{m}_{i'jk}, \tag{6}$$

where $(d_{ii'})$ is a discrete representation for the operator $\partial^2/\partial x^2$.

The most common representation for the exchange energy involves a three term approximation to the second derivative in (5), namely

$$f''(x_k) = \frac{1}{h^2}\,(f_{k-1} - 2f_k + f_{k+1}) + O(h^2), \tag{7}$$

for $f \in C^4[x_k - h, x_k + h]$. This expression involves the center point x_k and its two nearest neighbors. Including the $\partial^2/\partial y^2$ and $\partial^2/\partial z^2$ terms expands the sum to three dimensions, and triples the neighbor count. Hence we call this the 'six neighbor method.'

At any point x where $f \notin C^4[x - h, x + h]$, and in particular at the boundaries of the simulation region (outside of which we assume $\mathbf{m} = \mathbf{0}$), the relation (7) cannot be used. We consider explicitly the case $x = x_1$ near the boundary $x = a$, but the general case is completely analogous.

Considering first the case with Neumann boundary conditions, where $f'(a)$ is given, Taylor series expansions about x_1 for f and f' yield

$$f''(x_1) = \frac{f_2 - f_1 - hf'(a)}{h^2} + O(h). \tag{8}$$

At equilibrium, in the absence of surface anisotropy or other boundary fields, the normal derivative of the magnetization at the boundary satisfies $\partial \mathbf{m}/\partial \hat{\mathbf{n}} = 0$ [4], which here means $f'(a) = 0$.

Compared to (7), the accuracy in (8) is $O(h)$ instead of $O(h^2)$. The symmetry of the samples about x_k in (7) results in cancellation of the $(x - x_k)^3$ terms in the Taylor expansion, which does not happen here. However, regardless of the number of samples n, there is only one edge term near $x = a$ where (8) is applied, and this term will be multiplied by the sample length h during the integration process. Thus the approximation in toto is $O(h^2)$. The approximation error in the interior, using (7), is $O(h^3)$ locally when considered part of the integration process, but the number of such terms is $n - 2 \approx (b - a)/h$, so the total approximation error in the interior is $O(h^2)$.

For Dirichlet boundary conditions, $f(a)$ is specified instead of $f'(a)$. Working as before, we obtain

$$f''(x_1) = \frac{4f_2 - 12f_1 + 8f(a)}{3h^2} + O(h). \tag{9}$$

The $8f(a)/(3h^2)$ term can be treated as an applied field concentrated in the x_1 discretization cell.

We can proceed similarly for an $O(h^4)$ method. A sixth order Taylor series expansion shows [5]

$$f''(x_k) = \frac{-f_{k-2} + 16f_{k-1} - 30f_k + 16f_{k+1} - f_{k+2}}{12h^2}$$
$$+ O(h^4), \tag{10}$$

for $f \in C^6[x_k - 2h, x_k + 2h]$. Expanding to three dimensions requires 12 neighboring samples of f, so we call this the '12-neighbor method.' Although less common than the 6-neighbor approach, this method has been considered before [6], [7], [8]. In this work we supply additional details and some new approaches to handling the boundary conditions.

The sampling requirements imply that (10) cannot be applied within two cells of a boundary. For Neumann boundary conditions, we find

$$f''(x_1) = \frac{-59f_1 + 64f_2 - 5f_3 - 32hf'(a)}{38h^2}$$
$$- \frac{11f'(x_1)}{19h} + O(h^3). \tag{11}$$

Analogous to the 6-neighbor setting, $O(h^3)$ accuracy here suffices to yield a fourth order method overall.

The $f'(x_1)$ quantity in (11) is an unknown value. However, f represents one component of $\mathbf{m}$ in (5), and $\mathbf{m} \cdot \partial \mathbf{m}/\partial x = 0$ at all points because of the constraint $\|\mathbf{m}\| = 1$. Thus, in (5) we can use

$$\mathbf{m} \cdot \partial^2 \mathbf{m}/\partial x^2\big|_{x_1} = \mathbf{m}_1 \cdot \frac{-59\mathbf{m}_1 + 64\mathbf{m}_2 - 5\mathbf{m}_3}{38h^2}$$
$$- \frac{16}{19h^2}\,\partial \mathbf{m}/\partial \hat{\mathbf{n}}\big|_a + O(h^3),$$

where typically $\partial \mathbf{m}/\partial \hat{\mathbf{n}}\big|_a = 0$. An alternative to using $f'(x_1)$ in (11) is to include an additional sample of f, say $f(x_4)$.

At cell x_2 we find

$$f''(x_2) = \frac{335f_1 - 669f_2 + 357f_3 - 23f_4}{264h^2}$$
$$+ \frac{1}{11h}f'(a) + O(h^3), \tag{12}$$

which makes explicit use of $f'(a)$. Solving for $f'(x_2)/h$ and adding the result to (12) yields

$$f''(x_2) = \frac{4f_1 - 15f_2 + 12f_3 - f_4}{6h^2}$$
$$- \frac{1}{h}f'(x_2) + O(h^3). \tag{13}$$

As before, the $f'(x_2)$ term can be dropped when considering the total integrand. Either (12) or (13) may be used to estimate $f''(x_2)$. In the simulation results below we used (12).

For Dirichlet boundary conditions,

$$f''(x_1) = \frac{-165f_1 + 40f_2 - 3f_3 + 128f(a)}{30h^2}$$
$$+ \frac{1}{h}f'(x_1) + O(h^3) \qquad (14)$$

and

$$f''(x_2) = \frac{175f_1 - 280f_2 + 147f_3 - 10f_4 - 32f(a)}{105h^2}$$
$$+ O(h^3), \qquad (15)$$

The $f'(x_1)$ term in the first equation can be ignored. The $f(a)$ terms can be treated as applied fields. In place of (15), one can use the relation (13), which is more convenient because then an applied field term arising from $f(a)$ is not required at x_2.

In a practical energy minimization scheme, e.g., conjugate-gradient, the energy is differentiated with respect to the discretized magnetization. From (6),

$$\frac{\partial \Phi_d}{\partial \mathbf{m}_{ijk}} = -2V_h \sum_{jk} w_j^y w_k^z \sum_{ii'} c_{ii'jk} \mathbf{m}_{i'jk}, \qquad (16)$$

where

$$c_{ii'jk} = \frac{1}{2}\left(A_{ijk}w_i^x d_{ii'} + A_{i'jk}w_{i'}^x d_{i'i}\right). \qquad (17)$$

Here $c_{ii'jk}$ is a symmetric bilinear form in i and i'. It is a general property of bilinear forms that $\mathbf{m}^T B \mathbf{m} = \mathbf{m}^T(B + B^T)\mathbf{m}/2$, so (6) can be rewritten as

$$\Phi_d = -V_h \sum_{jk} w_j^y w_k^z \sum_{ii'} c_{ii'jk} \mathbf{m}_{ijk} \cdot \mathbf{m}_{i'jk}. \qquad (18)$$

In the remainder of this section we consider the case where A is constant. If we factor A out of the integral (2), so $c_{ii'jk} = c_{ii'}$, we can rewrite the inner sum in (18) as $\mathbf{m}^T C \mathbf{m}$, where $C = (c_{ii'})$. The norm constraint, $\|\mathbf{m}\| = 1$, implies that any modifications along the diagonal of the matrix C only change the computed energy by a constant offset. Since we are interested in energy differences and minima, such a change is not significant; moreover, adjusting the diagonal values so the rows sum to zero yields better numerics because there is less roundoff error when the neighbor-to-neighbor magnetization variation is small [9].

For the 6-neighbor method with Neumann boundary, the C resulting from (11) automatically satisfies these conditions. However, for Dirichlet boundary conditions the matrix arising from (9) is asymmetric; making the above adjustments yields

$$C = \begin{bmatrix} -7/6 & 7/6 & & & \\ 7/6 & -13/6 & 1 & & \\ & 1 & -2 & 1 & \\ & & & & \ddots \end{bmatrix}, \qquad (19)$$

where the bottom right hand corner of the matrix is symmetric about the cross diagonal with the upper left hand corner, i.e., the matrix is centro-symmetric [10]. There is in addition an effective boundary cell applied field, from (9).

For the 12-neighbor methods, the boundary corrections, including the w_i^x terms for the $O(h^4)$ integration method (3), affect the first 5 rows of C. Table I presents the coefficients of C. These are pentadiagonal matrices; non-zero entries are found by symmetry of the entries in this table about either diagonal, or otherwise from the general interior formulae $c_{k,k} = -5/2$, $c_{k,k\pm 1} = 4/3$, $c_{k,k\pm 2} = -1/12$.

In addition to convergence as a function of h, one can also look at the number of iterates of an energy minimization method, say conjugate-gradient, needed to converge for a fixed h. We call this 'iterative convergence.' To a large extent, the iterative convergence can be predicted from an eigenvalue analysis of C. We computed numerically the eigenvalues of $-C$ for modest sizes (up to $n = 19$), and found them to lie in the range $[0, 4)$ for the 6-neighbor methods, and inside $[0, 16/3)$ for the 12-neighbor methods. The 0 eigenvalue corresponds to the uniformly magnetized state, which is minimal exchange energy. The upper limit corresponds to a bulk $+1$, -1, $+1$, ... alternating state, which is maximal exchange energy. In practice we found all of the exchange energy formulations considered above to have similar iterative convergence behavior.

C. 26-neighbor exchange energy

The third approach uses exchange energy representation (1) instead of (2). The magnetization between the discretization points is approximated using a trilinear interpolation of nearby grid points, with basis functions $\{1, x, y, z, xy, xz, yz, xyz\}$. Given this piecewise polynomial representation for $\mathbf{m}(x, y, z)$, and assuming constant A, formula (1) can be computed analytically. Similar methods are employed in finite-element micromagnetics [11], [12].

The total exchange energy is found to be

$$\frac{AV_h}{36} \sum_{ijk} \sum_{i'j'k'} c_{ijki'j'k'}(\mathbf{m}_{ijk} - \mathbf{m}_{i'j'k'}) \cdot \mathbf{m}_{ijk} \qquad (20)$$

where the coefficients $c_{ijki'j'k'}$ are specified in Table II. There are 26 non-zero terms, so this is a '26-neighbor' method. Cells $\mathbf{m}_{i'j'k'}$ outside the simulation volume are handled by reflecting $\mathbf{m}$ across the boundary, which is equivalent to specifying $\partial \mathbf{m}/\partial \hat{\mathbf{n}} = 0$ at the boundary. This is an $O(h^2)$ method. We have not considered Dirichlet boundary conditions for this method.

For cubic cells, $h_x = h_y = h_z = h$, and the above expressions for the coefficients $c_{ijki'j'k'}$ simplify to $c_{ijk\bar{i}jk} = c_{ijki\bar{j}k} = c_{ijkij\bar{k}} = 0$, $c_{ijk\bar{i}\bar{j}k} = c_{ijk\bar{i}j\bar{k}} = c_{ijki\bar{j}\bar{k}} = 6/h^2$, and $c_{ijk\bar{i}\bar{j}\bar{k}} = 3/h^2$. If additionally we assume there is no variation in $\mathbf{m}$ along the z-axis, then we obtain the two-dimensional '8-neighbor dot product' studied previously [1].

III. Simulation Results

The exchange energy formulations described above were implemented within the OOMMF micromagnetic package [13], which was used to produce the following results.

We first compared the exchange representations for a head-to-head transverse wall in a thin film strip. Only exchange and anisotropy energies were included. The magnetization was held in the film plane by a strong easy-plane anisotropy, and the wall center was pinned by a uniaxial anisotropy directed along the strip axis, with spatially varying K_u of the form $r^2/(1+r^2)$, where r is the distance from the center of the strip. In order to get $O(h^4)$ convergence in the anisotropy calculation, we used the integration weights from (3) to compute the anisotropy energy. Using Neumann $\partial\mathbf{m}/\partial\hat{\mathbf{n}} = 0$ boundary conditions, the 6- and 26-neighbor methods showed $O(h^2)$ convergence, while the 12-neighbor method obtained $O(h^4)$ convergence, as expected.

Fig. 1 compares convergence of the 6- and 12-neighbor methods on two turns of a uniform 1D magnetization spiral. Here γ is the (uniform) angle between adjacent $\mathbf{m}_k$; $\gamma = 720°/n$. When the proper Dirichlet boundary conditions are applied, the convergence rates are second and fourth order, respectively. However, since the ends of the spiral are held fixed, $\partial\mathbf{m}/\partial\hat{\mathbf{n}} \neq 0$. The consequence of applying incorrect boundary conditions is seen in the top two curves—the convergence drops to first order. For this 1D simulation, the 6- and 26-neighbor methods are equivalent.

μMAG Standard Problem No. 3 [14] is studied in Fig. 2. In this 3D problem, the equilibrium configurations of a cube with easy-axis anisotropy K_u directed along a cube principal axis are calculated. The case we considered was a vortex magnetization configuration with cube edge length L set to $8.5\,l_{ex}$, where l_{ex} is the magnetostatic exchange length $\sqrt{2A/(\mu_0 M_s^2)}$. We found the reduced total energy density in the equilibrium state to be $0.3015 \times \mu_0 M_s^2/2$, which is comparable to values reported by other researchers [14]. Unlike the other examples, this problem includes self-magnetostatic energy. Since our implementation does not include an $O(h^4)$ representation for self-magnetostatic energy, it is not surprising that the convergence rates

are second order. Even so, for a given cell size h, the error from the 12-neighbor method is almost half that from the 6-neighbor method. We also performed tests where the magnetization was subsampled from the equilibrium configuration of the finest discretization. In that case, with the magnetization held fixed, the 12-neighbor method attains $O(h^4)$ convergence as the subsampling rate is varied.

It is also important to consider discretization induced effects on magnetization structures [1], [15]. Fig. 3 examines the effects of cell size on vortex motion. In this study, a vortex configuration is centered in a thin film 132 nm square element, with Py material properties ($A = 13$ pJ/m, $M_s = 800$ kA/m). Self-magnetostatic energy is simulated with a strong easy-plane uniaxial anisotropy, $K_u = \mu_0 M_s^2$. This is an unstable configuration in the continuum setting; the slightest in-plane applied field suffices to push the vortex core away from the center position. In practice, however, divots in the energy surface produced by the discretization pin the vortex in place. One measure of this effect is the field, H_{pin}, required to unpin the vortex. As seen in Fig. 3, the 26-neighbor method has significantly smaller H_{pin} for $h > l_{ex}$, but otherwise the 12-neighbor method dominates.

We also tested Néel wall collapse [15], and found that the 12-neighbor method to be somewhat more resistant to this discretization artifact than the 6- or 26-neighbor methods.

IV. Conclusions

We have examined 3 formulations for exchange energy, with general Neumann and Dirichlet boundary conditions. As a function of the discretization cell size h, the error for the 6- and 26-neighbor methods is $O(h^2)$, while for the 12-neighbor it is $O(h^4)$. When considering the convergence of equilibrium states, the rate is limited by the slowest convergence among all the energy terms. Even in this case the 12-neighbor method can yield significantly smaller errors. The 12-neighbor method is also found to be generally preferable in our tests of discretization induced vortex pinning, although the 26-neighbor method should be considered if one is forced to work with coarse grids.

References

[1] M.J. Donahue, R.D. McMichael, Physica B 233 (1997) 272.

[2] P.J. Davis, P. Rabinowitz, Methods of Numerical Integration, Academic Press, Orlando, 1984.

[3] J. Stoer, R. Bulirsch, Introduction to Numerical Analysis, Springer-Verlag, New York, 1993.

[4] W.F. Brown, Jr., Micromagnetics, Wiley Interscience, New York, 1963.

[5] M. Abramowitz, I.A. Stegun (Eds.), Handbook of Mathematical Functions, U.S. NBS, Washington D.C., 1970.

c_{ij}	Neumann	Dirichlet
c_{11}	-325703/240768	-2639/2880
c_{12}	39257/26752	73/72
c_{13}	-1255/10944	-281/2880
c_{22}	-643747/240768	-79/32
c_{23}	16297/12672	113/72
c_{24}	-337/4224	-11/96
c_{33}	-196421/80256	-1319/480
c_{34}	49/36	49/36
c_{35}	-49/576	-49/576
c_{44}	-32077/12672	-719/288
c_{55}	-1439/576	-1439/576

TABLE I

CORNER COEFFICIENTS FOR $O(h^4)$ INTERACTION MATRICES, FOR $\partial\mathbf{m}/\partial\hat{\mathbf{n}} = 0$ NEUMANN AND DIRICHLET BOUNDARY CONDITIONS WITH CONSTANT EXCHANGE COEFFICIENT A.

$c_{ijk\bar{i}jk}$	$\frac{16}{h_x^2} - \frac{8}{h_y^2} - \frac{8}{h_z^2}$
$c_{ijki\bar{j}k}$	$-\frac{8}{h_x^2} + \frac{16}{h_y^2} - \frac{8}{h_z^2}$
$c_{ijkij\bar{k}}$	$-\frac{8}{h_x^2} - \frac{8}{h_y^2} + \frac{16}{h_z^2}$
$c_{ijk\bar{i}\bar{j}k}$	$\frac{4}{h_x^2} + \frac{4}{h_y^2} - \frac{2}{h_z^2}$
$c_{ijk\bar{i}j\bar{k}}$	$\frac{4}{h_x^2} - \frac{2}{h_y^2} + \frac{4}{h_z^2}$
$c_{ijki\bar{j}\bar{k}}$	$-\frac{2}{h_x^2} + \frac{4}{h_y^2} + \frac{4}{h_z^2}$
$c_{ijk\bar{i}\bar{j}\bar{k}}$	$\frac{1}{h_x^2} + \frac{1}{h_y^2} + \frac{1}{h_z^2}$

TABLE II

COEFFICIENTS FOR THE 26-NEIGHBOR EXCHANGE ENERGY FORMULATION, EQ. (20). HERE $\bar{i} = i \pm 1$, $\bar{j} = j \pm 1$, $\bar{k} = i \pm 1$, AND $c_{ijki'j'k'} = 0$ OTHERWISE.

[6] P. Trouilloud, J. Miltat, J. Magn. Magn. Mater. 66 (1987) 194.
[7] D.V. Berkov, K. Ramstöck, A. Hubert, Phys. Stat. Sol. (a) 137 (1993) 207.
[8] M. Labrune, J. Miltat, J. Magn. Magn. Mater. 151 (1995) 231.
[9] M.J. Donahue, D.G. Porter, R.D. McMichael, J. Eicke, J. Appl. Phys. 87 (2000) 5520.
[10] J.M. Marin, T. Dhorne, Statistics 37 (2003) 85.
[11] W.J. Chen, D.R. Fredkin, and T.R. Koehler, IEEE Trans. Magn. 29 (1993) 2124.
[12] J. Fidler, T. Schrefl, J. Phys. D: Appl. Phys. 33 (2000) R135.
[13] M.J. Donahue, D.G. Porter, OOMMF User's Guide, NISTIR 6376, NIST, Gaithersburg, MD, 1999.
[14] R.D. McMichael, M.J. Donahue, <URL: http://www.ctcms.gov/~rdm/mumag.html>.
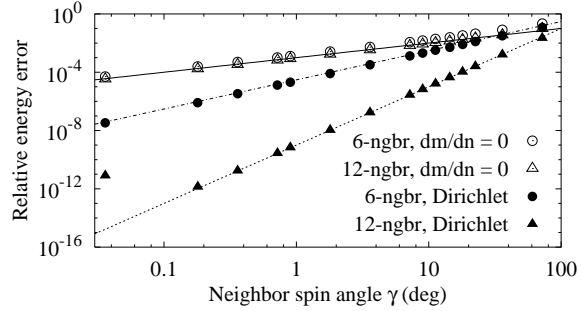[15] M.J. Donahue, J. Appl. Phys. 83 (1998) 6491.

Fig. 1. Exchange energy error for a two period uniform magnetization spiral. The fitted lines are, top to bottom, $10^{-3}\gamma$, $3 \times 10^{-5}\gamma^2$, and $10^{-9}\gamma^4$.
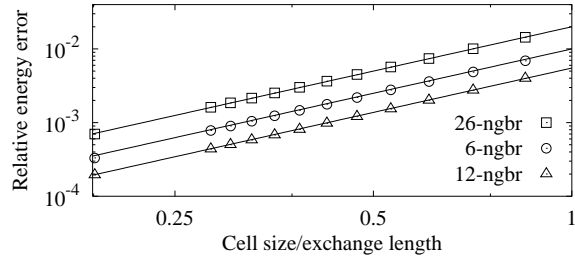

Fig. 2. Total energy error for μMAG Standard Problem No. 3. The fitted lines are, top to bottom, $0.02\Delta^2$, $0.01\Delta^2$, and $5.5 \times 10^{-3}\Delta^2$, where $\Delta = h/l_{\mathrm{ex}}$. The reference energy is obtained by extrapolating to $h = 0$.
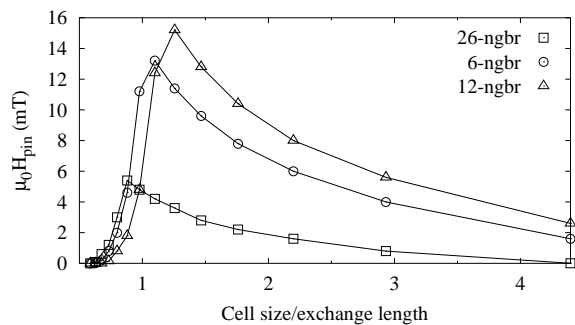

Fig. 3. Applied field required to unpin a vortex as a function of discretization cell size.